Assessing Real-Time RR-QT Frequency-Domain Measures of Coupling and Causality through Inhomogeneous Point-Process Bivariate Models

G. Valenza[1,2,*], M. Orini[3,*], L. Citi[4], A. Minchole[5], E. Pueyo[6], P. Laguna[6], R. Barbieri[1,**]

Abstract— **Ventricular repolarization instability is known to be related to arrhythmogenesis and increased risk of sudden cardiac death. These repolarization dynamics are linked to the distance between T-wave and Q-wave occurrances (QT) on the ECG, and they are coupled with R-wave to R-wave interval variability (RRV). Several efforts have been dedicated to the analysis of QT-RR interactions in order to provide both a quantification of the coupling and estimates of intrinsic repolarization dynamics. However, a methodology able to quantify dynamic changes in repolarization variability unrelated to RRV dynamics is still needed. In this study, we propose a bivariate model embedded within a multiple inhomogeneous point-process framework to obtain time-varying tracking of (causal) interactions between QT variability (QTV), a marker of repolarization variability, and RRV. Data from 15 healthy subjects undergoing a tilt table test were analyzed. Our results demonstrate that the model effectively captures the time-varying mutual QTV-RRV interactions. The analysis of time-varying coherence confirms that head-up tilt is associated with a decrease in linear QTV-RRV coupling, while time-varying directed coherence shows that intrinsic QTV becomes more prominent during head-up tilt.**

I. Introduction

QT variability (QTV), i.e. the temporal difference between consequent Q and T waves in the ECG, is a marker of ventricular repolarization instability [1]. QTV is influenced by autonomic nervous system (ANS) activity and several other non-autonomic factors [2]. Increased QTV is associated with an increased risk of sudden cardiac death [3], [4]. Heartbeat dynamics, reflected in R-R interval variability (RRV), significantly contributes to QTV [5]. However, the contribution of RRV to QTV may confound and reduce the predictive value of intrinsic QTV [4], i.e. the temporal fluctuations of ventricular repolarization unrelated to RRV and ANS control of the sinus node [1]. To this extent, the analysis of dynamic QTV-RRV interactions could provide a novel understanding of autonomic regulation of the cardiovascular function as well as more accurate measures of the intrinsic QTV.

* These authors equally contributed to this work.
** Corresponding author.

The research leading to these results has received partial funding from the Department of Anesthesia, Critical Care & Pain Medicine, Massachusetts General Hospital, Harvard Medical School, Boston, MA, USA, from projects TEC2010-21703-C03-02 and TEC2010-19410 from MICINN, Spain, and Ramn y Cajal fellowship, MICINN, Spain.

1. Department of Anesthesia, Critical Care & Pain Medicine, Massachusetts General Hospital, and Harvard Medical School, Boston, MA, USA, and Massachusetts Institute of Technology, Cambridge, MA, USA (* e-mail: {gvalenza,barbieri}@neurostat.mit.edu).
2. Research Center E. Piaggio and also Department of Information Engineering, University of Pisa, Pisa, Italy.
3. Institute of Cardiovascular Science, University College of London, UK
4. School of Computer Science and Electronic Engineering, University of Essex, Colchester, UK.
5. Computer Science Dptm, University of Oxford, UK.
6. GTC, Aragón Institute of Engineering Research, Universidad de Zaragoza, Spain, and CIBER-BBN, Zaragoza, Spain.

Recently, it has been shown that RRV-QTV coupling can significantly change under different physiological and pathological conditions, such as reduced vagal activity [5], aging [6], and presence of acute myocardial infarction [7]. Estimates of RRV-QTV coupling have been achieved through bivariate linear models [5], [6], [8]. This parametric representation allows for the calculation of frequency-domain measures of coupling (e.g., coherence (COH), partial coherence) and causality (e.g., directed coherence (DC), partial directed coherence) providing estimates of information transfer in physiological processes [9]. Time-varying methods for the detection of coupling or causality are strongly recommended when dealing with non-stationary data (such as RR and QT series) which are expected to reflect connectivity patterns with significant changes over time [9]. Therefore, in this study we investigate the temporal changes in COH and DC, along with auto- and cross-spectral measures. We further address the real-time R-wave, Q-wave, and T-wave occurrences by embedding a standard bivariate model into a multiple inhomogeneous point-process framework. Of note, the QT interval is approximated by the RT interval [10], i.e., the temporal distance going from the R-peak and the end of the T-wave in the ECG. Given that RT refers to the waiting time between two events, RT dynamics can also be suitably modeled using a point-process framework [11].

The bivariate model accounts for the mutual linear interaction between RT and RR dynamics to describe the first order moment of two coupled inverse-Gaussian probability distributions. The two probability functions follow independent temporal dynamics for the instantaneous parameter estimation [12], thus accounting for a real-time assessment of the RRV-RTV coupling. Other advantages defined by the point-process theory include model goodness-of fit and no need for interpolation methods on the series [13]–[16]. The proposed methodology is tested using data recorded from healthy volunteers undergoing head up tilt table tests. We first quantify temporal changes in spectral features and coherence, and then we use DC indices to quantify RRV linear contribution to RTV, and assess how intrinsic RTV changes during tilt. We investigate the newly derived instantaneous measures of coupling and causality through variability measures of the estimated indices along the experimental sessions (i.e., resting and tilted state). Averaged results are compared with previous findings reporting on the powers of the RR and RT spectral components and coherence [9].

II. Methodology of Statistical Signal Processing

A. Multiple Inhomogeneous Point-Process Framework for RR-RT Cardiovascular Dynamics

The point-process framework defines the probability of having an event at each moment in time. In this study, we define two parallel Inverse Gaussian-based inhomogeneous

978-1-4244-7929-0/14/$26.00 ©2014 IEEE

point-processes modeling the RR and RT dynamics, whose interaction is implemented through the mutual linear dependency of RR and RT autoregressive terms on the definition of the first order moments. Let us consider a set of R-wave events $\{u_j\}_{j=1}^{J}$, detected from the ECG, such that $\mathrm{RR}_j = u_j - u_{j-1} > 0$ denotes the j^{th} R-R interval. We also define $t \in (0,T]$ as the observation interval, $0 \leq u_1 < \cdots < u_k < u_{k+1} < \cdots < u_K \leq T$ as the times of the events, and $N(t) = \max\{k : u_k \leq t\}$ as the sample path of the associated counting process. Its differential, $dN(t)$, denotes a continuous-time indicator function, where $dN(t) = 1$ when there is an event, or $dN(t) = 0$ otherwise. The left continuous sample path is defined as $\widetilde{N}(t) = \max\{k : u_k < t\}$.

The probability density function of the waiting time $t - u_j$ until the next R-wave event is characterized by the following inverse-Gaussian model [13]:

$$f_{RR}(t|\mathscr{H}_t^{\mathrm{RR}}, \xi^{\mathrm{RR}}(t)) = \left[\frac{\xi_0^{\mathrm{RR}}(t)}{2\pi(t-u_j)^3}\right]^{\frac{1}{2}} \times \exp\left\{-\frac{1}{2}\frac{\xi_0^{\mathrm{RR}}(t)[t-u_j-\mu_{\mathrm{RR}}(t,\mathscr{H}_t^{\mathrm{RR}},\xi^{\mathrm{RR}}(t))]^2}{\mu_{\mathrm{RR}}(t,\mathscr{H}_t^{\mathrm{RR}},\xi^{\mathrm{RR}}(t))^2(t-u_j)}\right\} \quad (1)$$

where $j = \widetilde{N}(t)$ is the index of the R-wave event before time t, $\mathscr{H}_t^{\mathrm{RR}} = (u_j, \mathrm{RR}_j, \mathrm{RR}_{j-1}, ..., \mathrm{RR}_{j-p+1}, \mathrm{RT}_j, \mathrm{RT}_{j-1}, ..., \mathrm{RT}_{j-q+1})$, $\xi^{\mathrm{RR}}(t)$ the vector of the time-varying parameters, $\mu_{\mathrm{RR}}(t, \mathscr{H}_t^{\mathrm{RR}}, \xi^{\mathrm{RR}}(t))$ the first-moment statistic (mean) of the distribution, and $\xi_0^{\mathrm{RR}}(t) > 0$ the shape parameter of the inverse Gaussian distribution.

As mentioned above, also the RT series can be modeled as an inhomogeneous point process [11]. We define $\{v_j\}_{j=1}^{J}$ as the ordered set of T-wave events whose fiducial point corresponds to the end of the wave. Then, let $\mathrm{RT}_j = v_j - u_j > 0$, as the j^{th} RT interval. Therefore, for $u_j < t < v_j$ it is possible to define:

$$f_{RT}(t|\mathscr{H}_t^{\mathrm{RT}}, \xi^{\mathrm{RT}}(t)) = \left[\frac{\xi_0^{\mathrm{RT}}(t)}{2\pi(t-u_j)^3}\right]^{\frac{1}{2}} \times \exp\left\{-\frac{1}{2}\frac{\xi_0^{\mathrm{RT}}(t)[t-u_j-\mu_{\mathrm{RT}}(t,\mathscr{H}_t^{\mathrm{RT}},\xi^{\mathrm{RT}}(t))]^2}{\mu_{\mathrm{RT}}(t,\mathscr{H}_t^{\mathrm{RT}},\xi^{\mathrm{RT}}(t))^2(t-u_j)}\right\} \quad (2)$$

Similarly to $f_{RR}(t|\mathscr{H}_t^{\mathrm{RR}}, \xi^{\mathrm{RR}}(t))$, the $f_{RT}(t|\mathscr{H}_t^{\mathrm{RT}}, \xi^{\mathrm{RT}}(t))$ definition has $\mathscr{H}_t^{\mathrm{RT}} = (u_j, \mathrm{RR}_j, \mathrm{RR}_{j-1}, ..., \mathrm{RR}_{j-p+1}, \mathrm{RT}_j, \mathrm{RT}_{j-1}, ..., \mathrm{RT}_{j-q+1})$, $\xi^{\mathrm{RT}}(t)$ the vector of the time-varying parameters, $\mu_{\mathrm{RT}}(t, \mathscr{H}_t^{\mathrm{RT}}, \xi^{\mathrm{RT}}(t))$ the first-moment statistic (mean) of the distribution, and $\xi_0^{\mathrm{RT}}(t) > 0$ the shape parameter of the inverse Gaussian distribution.

B. Modeling the First Order Moment of the Two Coupled Inhomogeneous Point-Processes

The link between the two coupled inhomogeneous point processes of the heartbeat and RT dynamics refers to the mathematical representation of the first order moment of the two inverse-Gaussian distributions. In this study, we adopted the following bivariate linear modeling:

$$\mu_{\mathrm{RR}}(t, \mathscr{H}_t^{\mathrm{RR}}, \xi^{\mathrm{RR}}(t)) = a_{11}(0,t) + \sum_{i=1}^{p} a_{11}(i,t)\,\mathrm{RR}_{\widetilde{N}(t)-i} + \sum_{i=1}^{q} a_{12}(i,t)\,\mathrm{RT}_{\widetilde{N}(t)-i} \quad (3)$$

$$\mu_{\mathrm{RT}}(t, \mathscr{H}_t^{\mathrm{RT}}, \xi^{\mathrm{RT}}(t)) = a_{22}(0,t) + \sum_{i=1}^{p} a_{21}(i,t)\,\mathrm{RR}_{\widetilde{N}(t)-i} + \sum_{i=1}^{q} a_{22}(i,t)\,\mathrm{RT}_{\widetilde{N}(t)-i} \quad (4)$$

with $a_{lk}(i,t)$ as the model coefficients which continuously characterize the dynamic RR-RT interactions. In particular, $a_{11}(i,t)$ and $a_{22}(i,t)$ account for the pure autoregressive contribution of the RR and RT dynamics, respectively, whereas $a_{12}(i,t)$ quantifies the linear contribution that the past RT events have on $\mu_{\mathrm{RR}}(t, \mathscr{H}_t^{\mathrm{RR}}, \xi^{\mathrm{RR}}(t))$, and $a_{21}(i,t)$ quantifies the linear contribution that the past RR events have on $\mu_{\mathrm{RT}}(t, \mathscr{H}_t^{\mathrm{RT}}, \xi^{\mathrm{RT}}(t))$, whereas i indicates the heartbeats.

We use the Newton-Raphson procedure to maximize the local log-likelihood defined in [13], [17], also using a waiting function $W(t-u_j) = 0.98^{(t-u_j)}$, with $t - u_j \leq 90$ s, to estimate the unknown time-varying parameter sets $\xi^{\mathrm{RR}}(t) = [\xi_0^{\mathrm{RR}}(t), a_{11}(0,t), a_{11}(1,t), ..., a_{11}(p,t), a_{12}(1,t), ..., a_{12}(q,t)]$ and $\xi^{\mathrm{RT}}(t) = [\xi_0^{\mathrm{RT}}(t), a_{22}(0,t), a_{22}(1,t), ..., a_{22}(p,t), a_{21}(1,t), ..., a_{21}(q,t)]$. Each model goodness-of-fit is evaluated by Kolmogorov-Smirnov (KS) distance and autocorrelation plot [13]. KS distance measures the largest distance between the cumulative distribution function of RR and RT series transformed to the interval (0,1] by using the time rescaling theorem [13], and the cumulative distribution function of a uniform distribution on (0,1]. The smaller the KS distances, the closer is the agreement between original RR and RT series and the proposed model.

C. Instantaneous Coupling and Causality Assessment of the dynamic RR-RT interactions

1) Time-frequency representations: Once the model's parameters have been derived, the instantaneous auto- and cross-spectra, as well as measures of COH and DC are calculated. Let us define the time-varying coefficient matrix $\mathbf{A}_i(t)$ as:

$$\mathbf{A}_i(t) = \begin{bmatrix} a_{11}(i,t) & a_{12}(i,t) \\ a_{21}(i,t) & a_{22}(i,t) \end{bmatrix} \quad (5)$$

This matrix can be projected from the time-lag domain to the frequency domain by Fourier transform:

$$\mathbf{A}(t,f) = \sum_{i=1}^{M} \mathbf{A}_i(t) e^{-j2\pi fi}, \quad \mathbf{H}(t,f) = [\mathbf{I} - \mathbf{A}(t,f)]^{-1} \quad (6)$$

where $\mathbf{H}(t,f)$ is the non-stationary transfer function of the system, and M is the order of the model $M = \max(p,q)$. Spectra, $S_{lk}(t,f)$, coherence $\gamma_{lk}(t,f)$ and directed coherence

$\gamma_{lk}^{DC}(t,f)$ are defined, for $\{l,k\} \in \{1,2\}$, as [9]:

$$S_{lk}(t,f) = \sum_{m=1}^{2} H_{lm}(t,f)\sigma_m^2(t)H_{km}^*(t,f) \quad (7)$$

$$\gamma_{lk}(t,f) = \frac{S_{lk}(t,f)}{\sqrt{S_{ll}(t,f)S_{kk}(t,f)}} \quad (8)$$

$$\gamma_{lk}^{DC}(t,f) = \frac{\sigma_k(t)H_{lk}(t,f)}{\sqrt{\sigma_1^2(t)|H_{l1}(t,f)|^2 + \sigma_2^2(t)|H_{l2}(t,f)|^2}} \quad (9)$$

where

$$\sigma_1(t) = \sqrt{\mu_{\mathrm{RR}}(t,\mathscr{H}_t^{\mathrm{RR}},\xi^{\mathrm{RR}}(t))^3(t)/\xi_0^{\mathrm{RR}}(t)};$$
$$\sigma_2(t) = \sqrt{\mu_{\mathrm{RT}}(t,\mathscr{H}_t^{\mathrm{RT}},\xi^{\mathrm{RT}}(t))^3(t)/\xi_0^{\mathrm{RT}}(t)} \quad (10)$$

are used as estimates of RR and RT variability, respectively. Coherence $|\gamma_{lk}(t,f)| = |\gamma_{kl}(t,f)|$ quantifies the strength of the RR-RT linear local coupling, whereas $|\gamma_{ll}(t,f)| = |\gamma_{kk}(t,f)| = 1$. Directed coherence $\gamma_{lk}^{DC}(t,f)$ represents the ratio between the part of $S_{ll}(t,f)$ due to process k and $S_{ll}(t,f)$ [9]. By definition, $|\gamma_{ll}^{DC}(t,f)|^2 + |\gamma_{lk}^{DC}(t,f)|^2 = 1$. In the proposed bivariate model, $|\gamma_{lk}^{DC}(t,f)|$ is equal to the magnitude of the partial directed coherence evaluated along the same direction $k \to l$ [9].

2) Estimation of Synchronization Indices: In order to estimate the instantaneous indices of synchronization, a time-varying spectral power calculated around the central frequency $f_{lk,B}(t)$ (i.e.,the instantaneous frequency of the LF or HF spectral peak of $|S_{lk}(t,f)|$) is defined as:

$$\Omega_{lk,B} = \left\{(t,f) \in [\mathbb{R}^+ \times B] \big| f = f_{jk,B}(t) \pm \frac{\Delta_F}{2}\right\} \quad (11)$$

where $B \in \{LF, HF\}$, LF$\in [0.04 - 0.15]$ Hz, HF$\in [0.15 - 0.40]$ Hz, TOT$\in [0 - 0.45]$ Hz, and $\Delta_F = 0.1$ Hz is the width of $\Omega_{lk,B}$. Moreover, $\Omega_{lk,TOT} = [0.04 - 0.45]$ Hz. Note that $f_{lk,B}(t)$ is estimated only if a spectral peak is detected in $f \in B$. The ratio between the power calculated in LF and HF bands are Bal_{RR} and Bal_{RT}, referring to the RR and RT estimates, respectively.

In addition, instantaneous powers, $P_{l,B}(t)$, coherence, $\gamma_{lk,B}(t)$, and directed coherence, $\gamma_{lk,B}^{DC}(t)$ are estimated as:

$$P_{l,B}(t) = \frac{1}{\Delta_F}\int_{\Omega_{lk,B}} S_{ll}(t,f)df \quad (12)$$

$$\gamma_{k,B}(t) = \max_{f_{lk,B}} \gamma_{lk}(t,f) \quad (13)$$

$$\gamma_{lk,B}^{DC}(t) = \max_{f_{lk,B}} \gamma_{lk}^{DC}(t,f) \quad (14)$$

along with their maxima $\hat{P}_{l,B}(t)$, $\hat{\gamma}_{lk,B}(t)$, $\hat{\gamma}_{lk,B}^{DC}(t)$, and average in frequency domain $\langle P_{l,B}\rangle(t)$, $\langle \gamma_{lk,B}\rangle(t)$, $\langle \gamma_{lk,B}^{DC}\rangle(t)$.

III. Experimental Protocol and Results

Extensive details on the experimental protocol are reported in [18], [19]. Briefly, ECG recordings were acquired from 15 healthy volunteers (age: 28.5± 2.8, 11 males) undergoing a head up tilt table test (standard lead V4 with a sampling frequency of 1000 Hz). Each recording comprised three stages: of 4 minutes in early supine position, 5 minutes tilted head up to an angle of 70 degrees, and 4 minutes back to supine position. Automatic algorithms for R-wave and T-wave detection were applied as described in [20]. Peak detection errors and ectopic beats were detected by means of our previously developed algorithm [14], based on the point-process statistics (local likelihood), and able to perform a real-time interval error detection and correction. Moreover, RR and RT series were manually checked.

TABLE I: Results estimated across subjects during the three stages of the experimental protocol.

Indices of RR-RT interaction				
Index	Rest	Head Up TIlt	Rest	p-value
μ_{RR} [ms]	991.2±58.4	788.6±81.1	984.0±41.2	$< 10^{-6}$
μ_{RT} [ms]	382.3±17.3	345.8±7.7	376.2±14.1	$< 10^{-6}$
σ^2_{RR} [ms]	605.4±318.3	172.2±155.8	520.0±284.7	< 0.02
σ^2_{RT} [ms]	5.8±1.7	7.6±2.4	7.3±2.8	< 0.04
Bal_{RR}	1.809±1.131	5.241±2.848	1.059±0.876	< 0.005
Bal_{RT}	0.485±0.218	0.621±0.273	0.430±0.184	*n.s.*
$\hat{\gamma}^{DC}_{12,LF}$	0.568±0.099	0.479±0.060	0.557±0.101	< 0.03
$\hat{\gamma}_{12,HF}$	0.929±0.049	0.849±0.062	0.916±0.052	< 0.003
$\langle\gamma^{DC}_{11,TOT}\rangle$	0.884±0.017	0.916±0.019	0.905±0.021	< 0.02
$\langle\gamma^{DC}_{12,TOT}\rangle$	0.412±0.020	0.352±0.025	0.369±0.043	< 0.01
$\langle\gamma^{DC}_{21,TOT}\rangle$	0.460±0.046	0.402±0.025	0.455±0.057	< 0.005
$\langle\gamma^{DC}_{22,TOT}\rangle$	0.848±0.030	0.872±0.019	0.860±0.028	< 0.005

p-values are from the Friedman non-parametric test
n.s. not significant

For each index X, the following steps were performed: 1) estimation of X through the series of each subject along the three stages (supine, tilted, supine); 2) considering the central 2 minutes of each stage, the median of X was calculated for each subject and for each stage; 3) inter-subject statistical analysis of X was performed through the Friedman non-parametric test under the null hypothesis of equal medians between the three experimental stages. All results in this paper referring to the inter-subject statistics are expressed as Median$(X) \pm$MAD(X), where MAD$(X) =$ Median$(|X -$Median$(X)|)$. The model orders $p = q = 7$ were chosen by preliminary KS goodness-of-fit analysis [13]. The sampling rate at which the model parameters were updated was set at 0.005 s, while all spectral indices were evaluated after having downsampled coefficients to 4 Hz.

We found that the two coupled point-process models performed a satisfactory prediction of the next RR and RT events in all subjects. KS distance values were 0.0900 ± 0.0176 for the RR series and 0.1508 ± 0.0322 for RT series. Table I shows the inter-subject statistics for some relevant indices. Figure 1 shows instantaneous trend and statistics of $\gamma^{DC}_{22,TOT}(t)$ which represents the intrinsic RT variability, i.e., the RT variability not linearly related to RRV. A significant decrease during the tilt phase was found in the means μ_{RR} and μ_{RT}, and variances σ^2_{RR} and σ^2_{RT}. No significant differences were found among the rest and tilt sessions for $P_{RR,LF}$, $P_{RR,TOT}$, and $P_{RT,LF}$, $P_{RT,HF}$, $P_{RT,TOT}$. However, the power $P_{RR,HF}$ significantly decreased and Bal_{RR} increased during the tilt session than in supine position. A significant decrease in the tilt phase with respect to the resting states was observed in $\hat{\gamma}^{DC}_{12,LF}$, $\hat{\gamma}_{12,HF}$ with p-value< 0.04. Significant changes were observed also in RR-RT causality measures such as $\langle\gamma^{DC}_{lk,TOT}\rangle$ with $\{l,k\} \in \{1,2\}$. Of note, the maxima $\hat{\gamma}^{DC}_{12,HF}$ resulted decreased during the tilt phase considering both its average and variability within the three sessions (p-value< 0.01).

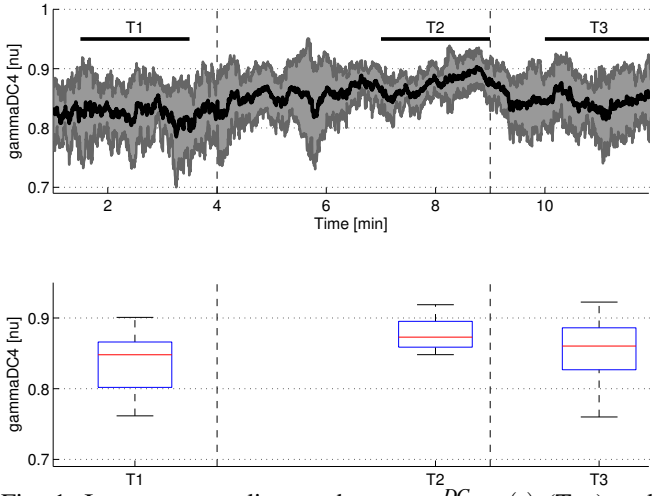

Fig. 1: Instantaneous direct coherence $\gamma^{DC}_{22,TOT}(t)$ (Top) and related box plots (bottom) during the three stages of the experimental protocol: first rest (T_1), head up tilt(T_2), and second rest (T_3).

IV. DISCUSSION AND CONCLUSION

In this study, we investigate a novel methodology to perform a real-time assessment of the RR-RT interaction using multiple inhomogeneous point-process models. In particular, a point-process framework including two separate probability structures is defined for the RR and RT dynamics, where their mutual interaction is considered in the definition of the first order moments. Goodness of fit measures such as KS and autocorrelation plots confirm that the proposed probabilistic method is suitable for proper prediction of the R- and T-waves by knowledge of past events detected from the surface ECG. In addition to monovariate instantaneous features defined in the time and frequency domain, we track the strength and directionality of RR-RT coupling through instantaneous coherence and directed coherence measures [9]. Our results show expected changes as a result of passive postural changes both in the time (μ_{RR}, μ_{RT}, σ^2_{RR}, σ^2_{RT}) and frequency ($P_{RR,HF}$ and Bal_{RR}) domains, as well as in $\gamma_{12,HF}$. The instantaneous causality reveals that, during tilt, RT variability due to heartbeat dynamics significantly decreases, whereas the intrinsic RT variability increases. Although this behavior is observed through the DC measures on the whole spectrum, the most significant changes are within the HF band. Interestingly, our results on $\langle\gamma^{DC}_{jk,TOT}\rangle$ demonstrate that RT variability does not affect RR variability as much as RR affects RT ($\langle\gamma^{DC}_{12,TOT}\rangle < \langle\gamma^{DC}_{21,TOT}\rangle$). Moreover, $\hat{\gamma}^{DC}_{12,HF}$ significantly decreased during the tilt phase (p-value< 0.01), suggesting a vagally-mediated mechanisms of contraction and repolarization of the ventricle as related to RR-RT coupling. The proposed framework confirms previous findings [3], [5]–[7], and further yields important information on the time-varying dynamics of RR-RT coupling. This consideration also confirms that time-varying RR-RT estimates provide valuable information for assessing ANS control and cardiovascular dynamics. Future work will be focused on devising novel nonlinear indices of causality within a bivariate point-process model.

REFERENCES

[1] E. Pueyo *et al.*, "A multiscale investigation of repolarization variability and its role in cardiac arrhythmogenesis." *Biophysical Journal*, vol. 101, no. 12, pp. 2892–2902, Dec 2011.

[2] S. Ahnve and H. Vallin, "Influence of heart rate and inhibition of autonomic tone on the qt interval." *Circulation*, vol. 65, no. 3, pp. 435–439, 1982.

[3] M. C. Haigney *et al.*, "QT interval variability and spontaneous ventricular tachycardia or fibrillation in the multicenter automatic defibrillator implantation trial (madit) ii patients," *Journal of the American College of Cardiology*, vol. 44, no. 7, pp. 1481–1487, 2004.

[4] L. Tereshchenko *et al.*, "Predictive value of beat-to-beat QT variability index across the continuum of left ventricular dysfunction competing risks of noncardiac or cardiovascular death and sudden or nonsudden cardiac death," *Circulation: Arrhythmia and Electrophysiology*, vol. 5, no. 4, pp. 719–727, 2012.

[5] A. Porta, E. Tobaldini, T. Gnecchi-Ruscone, and N. Montano, "RT variability unrelated to heart period and respiration progressively increases during graded head-up tilt," *American Journal of Physiology-Heart and Circulatory Physiology*, vol. 298, no. 5, pp. H1406–H1414, 2010.

[6] M. Baumert, B. Czippelova, A. Porta, and M. Javorka, "Decoupling of QT interval variability from heart rate variability with ageing," *Physiological Measurement*, vol. 34, no. 11, p. 1435, 2013.

[7] E. Nahshoni, B. Strasberg, E. Adler, S. Imbar, J. Sulkes, and A. Weizman, "Complexity of the dynamic QT variability and RR variability in patients with acute anterior wall myocardial infarction: a novel technique using a non-linear method," *Journal of Electrocardiology*, vol. 37, no. 3, pp. 173–179, 2004.

[8] R. Almeida, S. Gouveia, A. Rocha, E. Pueyo, J. Martinez, and P. Laguna, "QT variability and HRV interactions in ECG: Quantification and reliability," *IEEE Transactions on Biomedical Engineering*, vol. 53, no. 7, pp. 1317–1329, 2006.

[9] L. Faes, S. Erla, and G. Nollo, "Measuring connectivity in linear multivariate processes: definitions, interpretation, and practical analysis," *Computational and Mathematical Methods in Medicine*, vol. 2012, 2012.

[10] A. Porta, G. Baselli, E. Caiani, A. Malliani, F. Lombardi, and S. Cerutti, "Quantifying electrocardiogram RT-RR variability interactions," *Medical and Biological Engineering and Computing*, vol. 36, no. 1, pp. 27–34, 1998.

[11] G. Valenza, M. Orini, *et al.*, "Assessing instantaneous QT variability dynamics within a point-process nonlinear framework," in *8th Conference of the European Study Group on Cardiovascular Oscillations*, 2014.

[12] M. Orini, L. Citi, and R. Barbieri, "Bivariate point process modeling and joint non-stationary analysis of pulse transit time and heart period," in *Proceedings of IEEE-EMBC*, 2012.

[13] R. Barbieri, E. C. Matten, A. R. A. Alabi, and E. N. Brown, "A point-process model of human heartbeat intervals: new definitions of heart rate and heart rate variability," *American Journal of Physiology-Heart and Circulatory Physiology*, vol. 288, no. 1, p. H424, 2005.

[14] L. Citi, E. Brown, and R. Barbieri, "A real-time automated point process method for detection and correction of erroneous and ectopic heartbeats," *Biomedical Engineering, IEEE Transactions on*, 2012.

[15] L. Citi, G. Valenza, and R. Barbieri, "Instantaneous estimation of high-order nonlinear heartbeat dynamics by lyapunov exponents," in *Proceedings of IEEE-EMBC*. IEEE, 2012.

[16] G. Valenza, L. Citi, and R. Barbieri, "Instantaneous nonlinear assessment of complex cardiovascular dynamics by laguerre-volterra point process models," in *Proceedings of IEEE-EMBC*. IEEE, 2013.

[17] G. Valenza, L. Citi, E. Scilingo, and R. Barbieri, "Point-process nonlinear models with laguerre and volterra expansions: Instantaneous assessment of heartbeat dynamics," *Signal Processing, IEEE Transactions On*, vol. 61, no. 11, pp. 2914–2926, 2013.

[18] M. Orini, P. Laguna, L. Mainardi, and R. Bailón, "Assessment of the dynamic interactions between heart rate and arterial pressure by the cross time–frequency analysis," *Physiological Measurement*, vol. 33, no. 3, p. 315, 2012.

[19] M. Orini, R. Bailón, P. Laguna, L. T. Mainardi, and R. Barbieri, "A multivariate time-frequency method to characterize the influence of respiration over heart period and arterial pressure," *EURASIP Journal on Advances in Signal Processing*, vol. 2012, no. 1, pp. 1–17, 2012.

[20] J. P. Martinez, R. Almeida, S. Olmos, A. P. Rocha, and P. Laguna, "A wavelet-based ECG delineator: Evaluation on standard databases," *IEEE Transactions on Biomedical Engineering*, vol. 51, no. 4, pp. 570–581, 2004.